

# Modeling of parasitic plasma under the divertor roof baffle

K. Matyash<sup>a,b,\*</sup>, R. Schneider<sup>b</sup>, X. Bonnin<sup>c</sup>, D. Coster<sup>d</sup>,  
V. Rohde<sup>d</sup>, H. Kersten<sup>a</sup>

<sup>a</sup> Institut für Niedertemperaturplasma, D-17489 Greifswald, Germany

<sup>b</sup> Max-Planck Institute für Plasmaphysik, EURATOM Association, D-17491 Greifswald, Germany

<sup>c</sup> CEA Cadarache, DRFC-SIPP, EURATOM Association, F-13108 St-Paul-lez-Durance, France

<sup>d</sup> Max-Planck Institute für Plasmaphysik, EURATOM Association, D-85748 Garching, Germany

## Abstract

In this paper we present results of numerical simulations of parasitic plasmas created by radiation under the divertor. The extended version of a 2d3v PIC-MCC code [K. Matyash, R. Schneider, A. Bergmann, W. Jacob, U. Fantz, P. Pecher, J. Nucl. Mater. 313–316 (2003) 434] is used for this purpose. The two mechanisms of formation of such plasmas are taken into account in the model: photoionization of the neutral gas in the volume, or electron-impact ionization by photoelectrons emitted from the surface. The photon fluxes necessary for creation of such plasmas are estimated. The magnitude of fluxes obtained within this model agrees with experimentally measured values and with estimates found in B2-Eirene calculations.

© 2004 Elsevier B.V. All rights reserved.

PACS: 52.25.Jm; 52.40.Kh; 52.55.Rk; 52.65.Rr

Keywords: Divertor plasma; Edge modeling; Radiation; Sheaths

## 1. Introduction

During the experimental campaign on the ASDEX Upgrade tokamak with the divertor DivII carbon–deuterium deposition layers were discovered below the roof baffle [1]. The hard brownish layers with low deuterium content were mostly found at surfaces located perpendicular to magnetic field lines. This suggested that the formation of these layers is dominated by charged particles which follow the magnetic lines. This idea was supported by shadowing patterns observed in such layers.

The dust particles embedded in the carbon layers led to the formation of a wake in the direction of the magnetic field (see Fig. 1). Probe measurements [2] have proven the existence of a low-temperature plasma below the roof baffle of the divertor DivIIb. The plasma with a density up to  $n_e = 10^{12} \text{cm}^{-3}$  and a temperature up to  $T_e = 15 \text{eV}$  was discovered below the divertor, in a region not connected with the core plasma via magnetic field lines (Fig. 1). It was found that the density of this plasma is strongly correlated with the radiation intensity measured below the divertor. This fact supported the assumption that the plasmas below the divertor are created by radiation [2]. There are two candidates for a formation of such ‘parasitic’ plasmas: photoionization of the neutral gas in the volume, or electron-impact ionization by photoelectrons emitted from the surface.

\* Corresponding author. Address: Friedrich-Ludwig-Jahn-Str. 19, 17489 Greifswald, Germany. Tel.: +49 03834 88 2400; fax: +49 03834 88 2409.

E-mail address: [knm@ipp.mpg.de](mailto:knm@ipp.mpg.de) (K. Matyash).

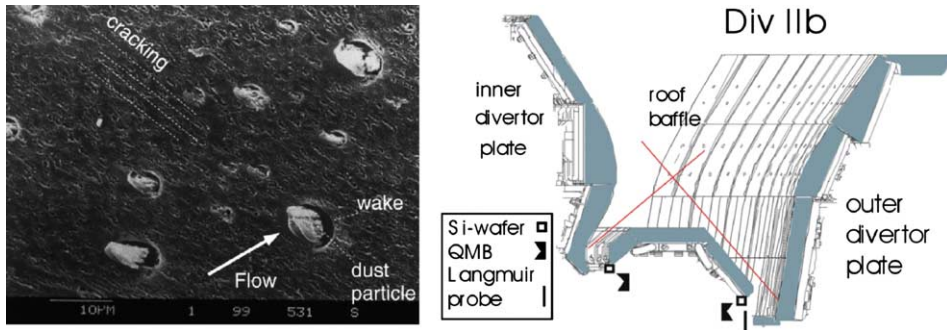


Fig. 1. The shadowing of the dust particles in the deposited C–D layers (left). Diagnostics used for detection of parasitic plasmas below the ASDEX Upgrade divertor DivIIb (right).

## 2. Simulation

In order to simulate the formation of ‘parasitic’ plasmas below the divertor roof baffle an extended version of the 2 dimensional in space, 3 dimensional in velocity space (2d3v) PIC MCC code [3] was used. The volume photoionization and surface photoeffect processes were added to the model.

The initial plasma parameters were chosen as  $n_{e0} = 10^{10} \text{ cm}^{-3}$  and  $T_{e0} = 20 \text{ eV}$ . A rectangular computational domain with a length of  $Y_{\text{max}} = 32\lambda_{D0} = 0.75 \text{ cm}$  and a width of  $X_{\text{max}} = 8\lambda_{D0} = 0.19 \text{ cm}$  was considered (here  $\lambda_{D0} = (\epsilon_0 k T_{e0} / n_{e0} e^2)^{1/2}$  is Debye radius). The wall, perpendicular to the direction  $Y$  was located at  $Y = Y_{\text{max}}$ . A uniform magnetic field  $B = 1.8 \text{ T}$  directed along the  $Y$  axis was applied. In the  $X$  direction, periodic boundary conditions were used, both for the particles and for the potential. At the target wall ( $Y = Y_{\text{max}}$ ) the potential was fixed at zero. At  $Y = 0$  the  $Y$  component of the electric field was set to zero. All particles hitting the target wall were absorbed, particles crossing the  $Y = 0$  were reflected back into the system. Neutral methane with a fixed density  $n_{\text{CH}_4} = 5 \times 10^{14} \text{ cm}^{-3}$  and temperature  $T_{\text{CH}_4} = 0.1 \text{ eV}$ , was considered as the background gas assuming a dominant chemical sputtering contribution. Such neutral density corresponds to values measured in the dome volume below the divertor of ASDEX Upgrade operating in the highly recycling mode [4]. In the simulation only the dynamics of the charged species was followed, the neutrals were treated as a fixed background. No neutral recycling on the target wall was included in the model.

For the sake of simplicity only Coulomb collisions between the charged particles and electron impact ionization of the methane were included in the simulation.

In calculations a grid size of  $\Delta x = \lambda_{D0}/2 = 0.017 \text{ cm}$  and a time step  $\Delta t = 0.2/\omega_{pe0} = 3.55 \times 10^{-11} \text{ s}$  was used. In order to speed up the simulation, the ion-to-electron mass ratio  $m_{\text{CH}_4^+}/m_e = 1600$  was chosen. The number of computational particles per Debye cell was chosen as  $N_d = 100$ .

In order to study the plasmas created by radiation, a constant flux of photons with energy  $E_v = 18.6 \text{ eV}$  and flux density  $j_v = 6.3 \times 10^{16} \text{ cm}^{-2} \text{ s}^{-1}$  directed along the  $Y$  axis was applied at  $Y = 0$ . Only the collisions of the photons with the methane were considered. Photoionization collisions were implemented via a Monte-Carlo collision algorithm [5]. A total photoionization cross-section  $\sigma_v = 4.2 \times 10^{-17} \text{ cm}^2$  [6] was used in the simulations. Correspondingly, the resulting secondary electrons had an energy  $E_e = E_v - E_i = 6 \text{ eV}$  (here  $E_i = 12.6 \text{ eV}$  is the methane ionization energy). The direction of the velocity of the secondary electrons was sampled from a uniform solid angle distribution in the electron-ion center of mass system.

For electron photoemission a wall material with a work function  $W = 4.2 \text{ eV}$  and a probability of photoemission  $\gamma_p = 0.3$  was chosen (representing stainless steel). The energy of the photoelectrons was chosen from a uniform energy distribution between  $0 \leq E_e < E_{\text{max}}$ , where the maximum energy of emitted electrons was  $E_{\text{max}} = E_v - W = 14.4 \text{ eV}$ . The direction of velocity of the photoelectrons was sampled from a uniform solid angle distribution within a hemisphere  $v_y < 0$ .

The results of the simulation are presented in Fig. 2. A plasma with density  $n_e \approx 10^{10} \text{ cm}^{-3}$  and temperature  $T_e \approx 1.7 \text{ eV}$  is created in the system due to the combined action of the neutral gas photoionization and the photoelectron emission from the wall. The electron density has a rather flat profile in the bulk region, abruptly increasing near the wall. This maximum of the electron density appears due to accumulation of the emitted electrons close to the wall.

In order to study the possibility of creating a low-temperature plasma due to photoemission of the energetic electrons from the wall, we performed a simulation in which the volume photoionization was switched off. In this case we found that in order to sustain the plasma with density about  $n_e \approx 10^{10} \text{ cm}^{-3}$  the photon flux had to be increased to  $j_v = 1.3 \times 10^{18} \text{ cm}^{-2} \text{ s}^{-1}$ . In Fig. 3 we present results of this simulation. The electron density, having the maximum at the wall monotonically decreases

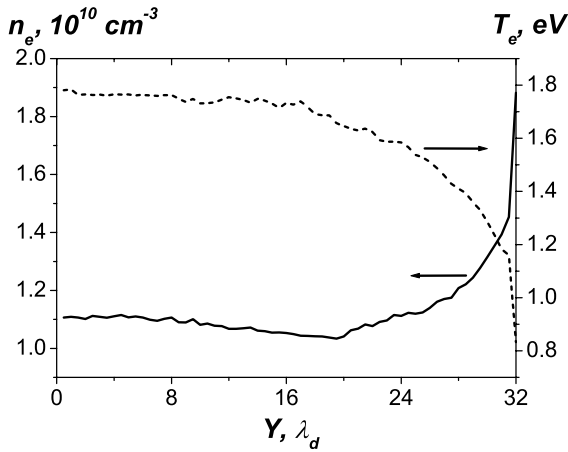


Fig. 2. Electron density and temperature profile for the plasma created by photons.

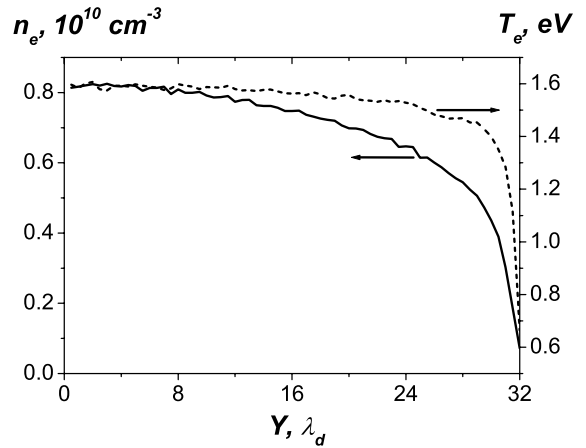


Fig. 4. Electron density and temperature profile for the plasma created due to photoionization of a neutral gas.

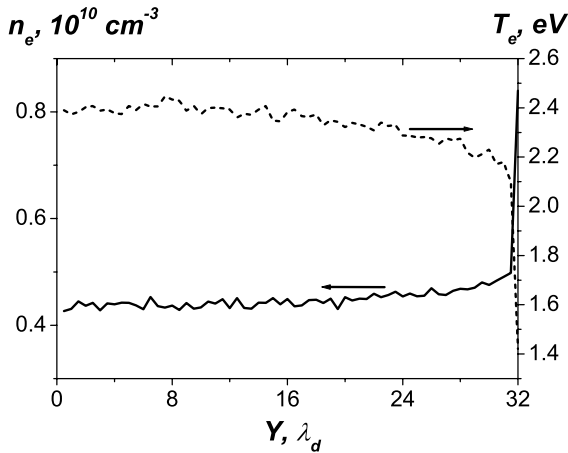


Fig. 3. Electron density and temperature profile for the plasma created due to surface photoemission.

toward  $Y = 0$ . The electron temperature becomes higher compared with the previous case (Fig. 2), having an average value of  $T_e \approx 2.3\text{eV}$ .

In Fig. 4 we present the results for a simulation in which only the photoionization of the neutral gas was considered (the photoemission from the wall was switched off). In this case the electron density has a profile which is typical for plasmas with volume ionization, decreasing from the bulk region toward the wall. The electron temperature profile is rather flat with an average value  $T_e \approx 1.6\text{eV}$ .

The radiation losses in the scrape-off layer of ASDEX Upgrade calculated with the B2-EIRENE code [7] are presented in Fig. 5. We can see that the radiation power is strongly increased in the tips of the divertor plates, where neutrals are trapped. The neutrals are re-

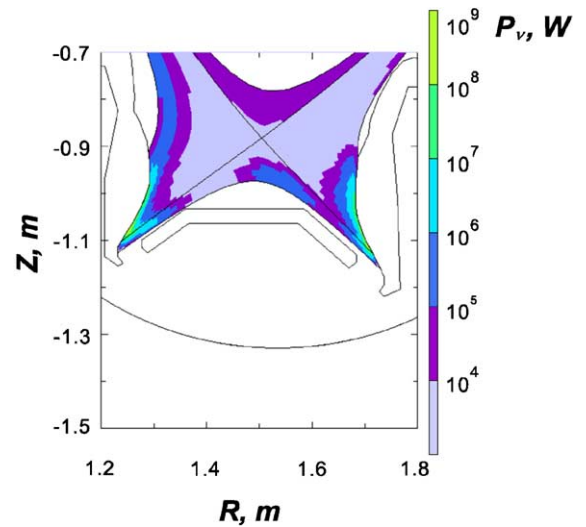


Fig. 5. Cell-integrated radiation losses calculated with B2-EIRENE for SOL of the ASDEX Upgrade with divertor DivII.

flected towards the hot plasma, where they get ionized and excited due to collisions with electrons [8]. The spectral emissivity for photons with energy  $h\nu > 18\text{eV}$ , integrated over the lines of sight of the spectrometer ROV [4] is plotted in Fig. 6. According to B2-EIRENE calculations the flux of the energetic photons under the divertor roof baffle is about  $j_\nu \sim 10^{16}\text{cm}^{-2}\text{s}^{-1}$  which is close to the flux value used in the PIC simulations. This supports the possibility of creating the low-temperature plasma observed below the roof baffle by radiation from the divertor.

According to the simulations, the direct photoionization of hydrocarbon molecules in the volume are

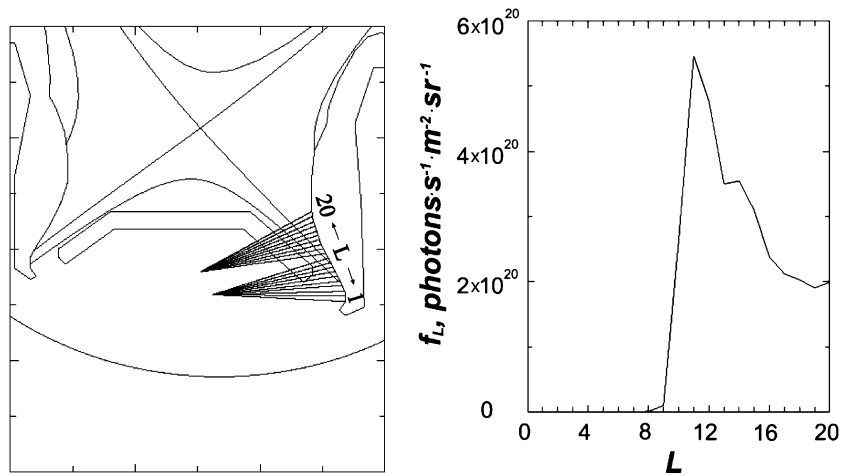


Fig. 6. Lines of the sights for divertor spectrometer ROV [4] (left); line-integrated spectral emissivity along the lines of sight of spectrometer ROV for photon energies  $h\nu > 18\text{eV}$  (right).

sufficient to sustain such ‘parasitic’ plasmas. The surface photoeffect alone would need about two order of magnitude higher radiation fluxes than observed experimentally.

### 3. Summary

The occurrence of parasitic low-temperature plasmas in areas far away from the SOL, such as below the divertor baffles in ASDEX-Upgrade [2], were proven to exist due to the emission of photoelectrons from surfaces and photoionization of neutral gas in the volume. The simulations have shown that photoionization of the neutral gas is a dominant mechanism of formation of such ‘parasitic plasmas’.

The photon fluxes necessary within our kinetic PIC model to sustain such plasmas were of the same order as experimental ones.

### References

- [1] V. Rohde, H. Maier, K. Krieger, R. Neu, J. Perchermaier, ASDEX Upgrade Team, *J. Nucl. Mater.* 290–293 (2001) 317.
- [2] V. Rohde, M. Mayer, ASDEX Upgrade Team, *J. Nucl. Mater.* 313–316 (2003) 337.
- [3] K. Matyash, R. Schneider, A. Bergmann, W. Jacob, U. Fantz, P. Pecher, *J. Nucl. Mater.* 313–316 (2003) 434.
- [4] J. Gafert, K. Behringer, D. Coster, C. Dorn, A. Kallenbach, R. Schneider, U. Schumacher, *J. Nucl. Mater.* 266–269 (1999) 365.
- [5] K. Matyash, Kinetic modeling of multi-component edge plasmas, PhD thesis, Ernst-Moritz-Arndt-University Greifswald, Germany, 2003.
- [6] C.J. Latimer, R.A. Mackie, A.M. Sands, N. Kouchi, K.F. Dunn, *J. Phys. B: At. Mol. Opt. Phys.* 32 (1999) 2667.
- [7] X. Bonnin, Private communication, 2003.
- [8] R. Schneider, H.S. Bosch, J. Neuhauser, D. Coster, K. Lackner, M. Kaufmann, *J. Nucl. Mater.* 241–243 (1997) 701.